Spatial and Temporal Structure of Chaotic Instabilities in an Electron-Hole Plasma in Ge

G. A. Held and Carson Jeffries
Department of Physics, University of California, Berkeley, California 94720, and Materials and Molecular Research Division, Lawrence Berkeley Laboratory, Berkeley, California 94720
(Received 13 June 1985)

Helical instabilities in an electron-hole plasma in Ge in parallel dc electric and magnetic fields are known to exhibit chaotic behavior. By fabricating probe contacts along the length of a Ge crystal we study the spatial structure of these instabilities, finding two types: (i) spatially coherent and temporally chaotic helical density waves characterized by strange attractors of fractal dimension $d \sim 3$, and (ii) beyond the onset of spatial incoherence, instabilities of indeterminately large fractal dimension $d > 8$. A transition between these two types of behavior is observed as the applied fields are increased.

PACS numbers: 72.30.+q, 05.45.+b, 47.25.–c, 71.35.+z

It is by now well established that the onset of turbulence in a wide range of physical systems can be characterized by temporal chaos.[1] That is, the evolution of these systems corresponds to motion in phase space along trajectories which are confined to a strange (fractal) attractor.[2] However, the relationship between low-dimensional chaos and spatial complexity is less well understood. Both experimental[3] and theoretical[4] continuum systems have been shown to exhibit temporally chaotic, spatially coherent behavior. However, there is as yet no clear experimental data on a system in which the breakup of spatial order can be characterized by low-dimensional chaotic dynamics. In this Letter we present results of experiments on the spatial and temporal dynamics of chaotic instabilities in an electron-hole (eh) plasma in Ge.

Spontaneous current oscillations in an eh plasma in parallel dc electric and magnetic fields are known to be the result of an unstable, traveling, screw-shaped helical density wave.[5,6] Held, Jeffries, and Haller[7] have found that when this instability is strongly excited by an increasing electric field, it will undergo both period-doubling and quasiperiodic transitions to low-dimensional temporal chaos. Experimentally, we vary the applied dc fields and record the dynamical variables $I(t)$, the total current passing through the sample, and $V(t)$, the voltage across it.

Given that these eh plasma instabilities do indeed exhibit chaos, we turn our attention to the question of spatial coherence within the instabilities. In particular, we would like to determine whether the observed chaotic states correspond to a temporally chaotic yet still spatially coherent helical plasma density wave or whether the onset of temporal chaos also corresponds to a breakup of spatial order within the density wave. By placing probe contacts along the length of our samples, we are able to monitor the local variations in plasma density. We have found two distinct types of behavior: (i) an essentially spatially coherent and temporally chaotic plasma density wave characterized by an attractor of fractal dimension $d \sim 3$, and (ii) a spatially incoherent wave with an unmeasurably large fractal dimension $d > 8$. Further, as the applied electric field E_0 is increased, we observe a transition between these two states—characterized by a partial loss of spatial order and a jump in fractal dimension. While the increase in fractal dimension from $d \sim 3$ to $d > 8$ is somewhat abrupt ($\Delta E_0/E_0 \sim 0.05$), the breakup of spatial order occurs gradually. It is physically reasonable that the onset of spatial incoherence (which increases the number of available degrees of freedom) would result in an increased fractal dimension. However, we cannot firmly establish that the onset of spatial disorder is *coincident* with the observed jump in fractal dimension; the possibility that these two events occur at comparable applied fields and yet are not directly related cannot be completely excluded.

Our experiments are performed on a $1 \times 1 \times 10\text{-mm}^3$ sample cut from a large single crystal of n-type Ge with a net donor concentration $N_D \sim 3.7 \times 10^{12}$ cm^{-3}.[7] A lithium-diffused n^+ contact (electron injecting) and a boron-implanted p^+ contact (hole injecting) were formed on opposite $1 \times 1\text{-mm}^2$ ends. Phosphor-implanted n^+ contacts were formed on two opposite $1 \times 10\text{-mm}^2$ faces. Using photolithography, we etched onto these two faces a pattern of eight pairs of contacts, 0.5 mm wide and spaced by 1 mm along the length of the sample. The voltage $V_i(t)$ across a pair of these contacts is a measure of the local variation in the plasma density.[6] The sample was lapped, etched, and then stored in dry air for 72 h to allow the surfaces to passivate.

When taking data, the sample is cooled to 77 K in liquid N_2 and connected in series with a 100-Ω resistance and a variable dc voltage, which both generates the eh plasma via double injection and creates the dc field E_0. The applied voltage V_{dc}, the applied magnetic field B_0, and the angle between the two fields θ comprise our control parameters; typically $\theta = 0 \pm 3°$. In practice, we fix B_0 and θ and sweep V_{dc}, while

© 1985 The American Physical Society

recording the dynamical variables $I(t)$, $V(t)$, and $V_i(t)$ which characterize the plasma behavior.

In different regions of parameter space (V_{dc}, B_0, θ) different types of transitions to turbulence are observed. For our system we make the operational definition that a transition to "weak" turbulence is one in which the transition from periodicity to chaos is followed by a transition back to periodicity as V_{dc} is increased further. All such transitions that we have observed occur over a small range (i.e., ~ 1 V) of V_{dc}, and in all such chaotic states there exists at least one fundamental peak which stands out clearly above the broad-band "noise" level of the power spectrum. The scenarios previously reported,[7] period-doubling and quasiperiodic transitions to chaos, were in parameter-space regions corresponding to transitions to weak turbulence.

The transition to weak turbulence which we consider here (taken with $B_0 = 11.15$ kG) is periodic at $V_{dc} = 5.50$ V, quasiperiodic at $V_{dc} = 5.59$ V, and chaotic at $V_{dc} = 5.71$ V. The power spectra and return maps (which are topologically equivalent to Poincaré sections[8]) for these three states are shown in Fig. 1. The structure within the return map at $V_{dc} = 5.71$ V strongly infers that the system is in a low-dimensional chaotic regime, and the following calculations of the fractal dimension confirm this.

We find the fractal dimension d of our plasma instability to be 1, 2, and 2.7 for the above periodic, quasiperiodic, and chaotic states, respectively. We use the following procedure to measure fractal dimensions of our system[9]: We begin by recording a data set of N values of the current at uniformly spaced time intervals [i.e., $I_n = I(t + n\tau)$, $n = 1, \ldots, N$] using a fast 12-bit analog-to-digital converter and an LSI-11/23 computer. From the data set $\{I_1, I_2, \ldots, I_N\}$ we construct $N - D + 1$ vectors $\mathbf{G}_n = (I_n, I_{n+1}, \ldots, I_{n+D-1})$ in a D-dimensional phase space; D is referred to as the embedding dimension of the reconstructed phase space $\mathbf{G}$.[8,9] Next, we compute the number of points on the attractor, $N(\epsilon)$, which are contained in a D-dimensional hypersphere of radius ϵ centered on a randomly selected vector $\mathbf{G}_m$. One expects $N(\epsilon)$ to scale as ϵ^d, where d is the fractal dimension of the attractor. This is repeated for hyperspheres centered on many different vectors $\mathbf{G}_m$, and a plot of the average $\log \bar{N}(\epsilon)$ vs ϵ is expected to have a slope d. This procedure is carried out for consecutive values $D = 2, 3, 4, \ldots,$ and an increasing number of data points N until the slope has converged. This is done to ensure that the embedding dimension is sufficiently large[10] (important if the dimension of the phase space is not known) and to discriminate against high-dimensional stochastic noise, not of deterministic origin.

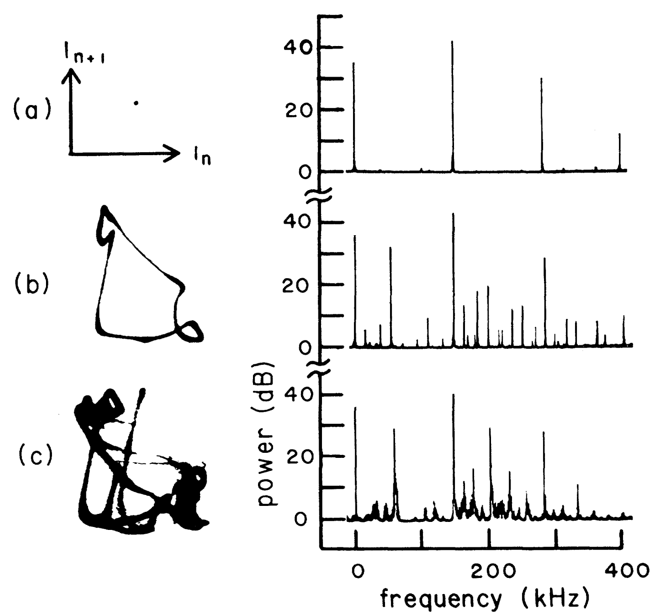

FIG. 1. Poincaré sections, I_n vs I_{n+1} (where $\{I_n\}$ is the set of local current maxima), and power spectra of the total current $I(t)$ at $B_0 = 11.15$ kG with increasing V_{dc}: (a) 5.50 V, periodic at $f_0 = 147$ kHz. (b) 5.59 V, quasiperiodic. (c) 5.71 V, chaotic. $I(t)$ is ac coupled and filtered to remove harmonic distortion.

To determine whether or not a weakly turbulent state is spatially coherent, we compare fluctuations in plasma density at different points along the sample. Quantitatively, we calculate a spatial correlation function, $C(r)$, defined as

$$C(r) = \left| \frac{2}{N} \sum_{n=1}^{N} V_i(n\tau) V_j(n\tau) \right|^{1/2}, \tag{1}$$

where $V_i(t)$ and $V_j(t)$ are the voltages across two pairs of contacts separated by a distance r, τ is the sampling interval, and N is a number large enough that $C(r)$ has converged, typically 20 000. We find that $C(r)$ is independent of τ.

For the periodic parameters above, the correlation function $C(r)$ for different spacings r between the pairs of probe contacts is plotted in Fig. 2(a). For each pair of contacts, the voltage difference $V_i(t)$ is periodic. By noting the phase shift between pairs of probes as a function of distance, we estimate that the spatial wavelength is $\lambda \approx 4.9$ mm. The theoretical correlation function for a traveling wave,

$$S(r) = \left[\frac{2}{T} \int_0^T \sin(\omega t) \sin(\omega t - 2\pi r/\lambda) dt \right]^{1/2}, \tag{2}$$

is also shown in Fig. 2(a); the periodic data points lie close to the theoretical curve. We believe that the observed deviations from theory are due to the harmonic components of the density wave, $2f_0$, $3f_0$, etc. {which are seen experimentally [Fig. 1(a)] but are not includ-

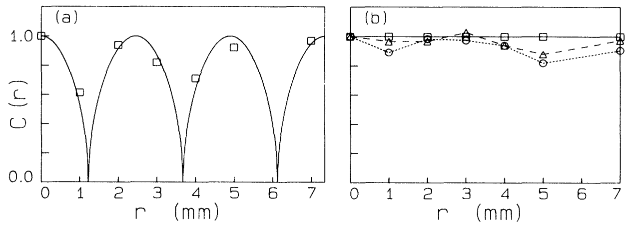

FIG. 2. (a) Comparison of measured values (squares) of the spatial correlation function, $C(r)$, Eq. (1), with the theoretical correlation function, $S(r)$, Eq. (2), computed for $\lambda = 4.9$ mm (solid line). Data were taken for the periodic state at $B_0 = 11.15$ kG, $V_{dc} = 5.50$ V with use of voltages from pairs of side probes separated by distance r. (b) Normalized comparison of measured values of spatial correlation function $C(r)$ for three data sets at $B_0 = 11.15$ kG: squares, periodic, $V_{dc} = 5.50$ V; triangles, quasiperiodic, $V_{dc} = 5.59$ V; circles, chaotic, $V_{dc} = 5.71$ V.

ed in Eq. (2)} and, possibly, to variations in probe sensitivity as well. Thus we conclude that the periodic oscillations are spatially coherent—not surprising, and consistent with previous experimental work.[6,11] In Fig. 2(b) we plot experimental correlation functions $C(r)$ for the quasiperiodic ($V_{dc} = 5.59$ V) and chaotic ($V_{dc} = 5.71$ V) states. In these plots, $C(r)$ for the periodic data has been normalized to unity at each distance r, and the quasiperiodic and chaotic data have been scaled accordingly. We find that the quasiperiodic and chaotic states both have correlation functions which approximately follow the periodic case. Therefore, we conclude that this weakly turbulent instability exhibits temporal chaotic behavior while remaining essentially a spatially coherent plasma density wave.

With sufficiently large applied electric and magnetic fields, we find that we can drive the plasma into a turbulent state from which it will not become periodic again as V_{dc} is increased further. Instead, all of the frequency peaks in the power spectrum merge into a single, broad, noiselike band. We classify this as a transition to "strong" turbulence. Such a transition is shown in Fig. 3. At $V_{dc} = 10.4$ V, $I(t)$ is simply periodic at $f_0 = 321$ kHz, with higher harmonics present as well [Fig. 3(a)]. At $V_{dc} = 11.6$ V, $I(t)$ is quasiperiodic and at $V_{dc} = 12.1$ V (not shown), the onset of broadband "noise" can be observed. At $V_{dc} = 13.8$ V [Fig. 3(b)], only a few of the peaks can be seen above the noise, and when $V_{dc} = 21.8$ V [Fig. 3(c)], only a very broad peak remains.

We find that this transition to strong turbulence is characterized by a partial loss of spatial coherence. In the right-hand column of Fig. 3, we plot the voltage traces across two pairs of probe contacts which are separated by $r = 4$ mm, for $V_{dc} = 10.4$, 13.8, and 21.8 V. In the periodic case, the wave is spatially coherent with a wavelength of approximately 8 mm (i.e., a 4-

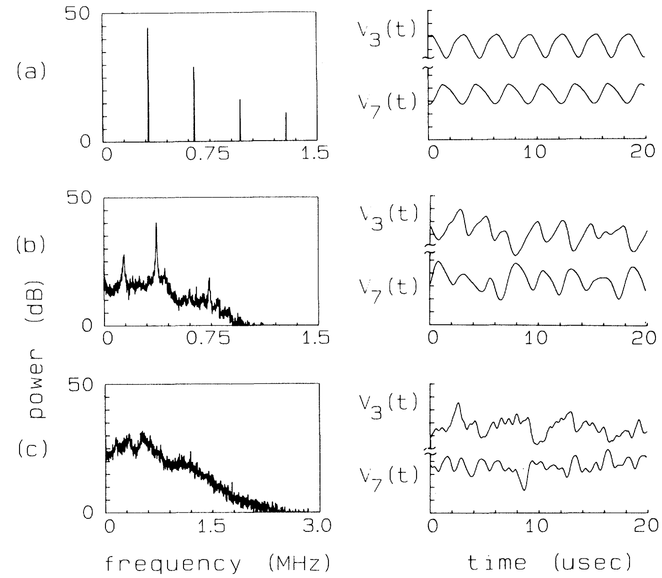

FIG. 3. Measured power spectra of $I(t)$ and measured voltages for two pairs of probe contacts separated by $r = 4$ mm: $V_3(t)$ and $V_7(t)$ correspond to probe pairs located 3 and 7 mm away from the p^+ contact, respectively. $B_0 = 11.15$ kG. (a) $V_{dc} = 10.4$ V, periodic at $f_0 = 321$ kHz. (b) $V_{dc} = 13.8$ V. (c) $V_{dc} = 21.8$ V.

mm separation corresponds to a 180° phase shift). At $V_{dc} = 13.8$ V we are just beyond the onset of the breakup of spatial order—the basic oscillatory pattern and the 180° phase shift are approximately maintained between the two traces, but changes in the shapes and spacings of the peaks can also be observed. For $V_{dc} = 21.8$ V, the wavelike structure of the traces as well as the readily observable spatial correlation are no longer present. We have not found a correlation function of analytic form which fits the data, in contrast to the case of Fig. 2.

We would like to determine whether this breakup of spatial order can be characterized by chaotic dynamics: Do the spatially uncorrelated states still correspond to motion in phase space along a low-dimensional strange attractor? We have as yet been unable to answer this question definitively. Just prior to the breakup of spatial coherence, $V_{dc} = 12.1$ V, the total current $I(t)$ of the system is characterized by a low-dimensional attractor; measurements of the fractal dimension yield $d = 2.5$ [Fig. 4(a)]. However, just after the onset of spatial disordering, $V_{dc} = 12.9$ V, the fractal dimension has increased to the point where we cannot calculate its value—we can only set a lower limit: $d \gtrsim 8$. This is shown in Fig. 4(b) where the slope has not converged with respect to either embedding dimension D or number of data points N. Figure 4(b) was taken with $N = 884\,000$ and required 50 h of central-processing-unit time on a Sun microcomputer. Fractal-

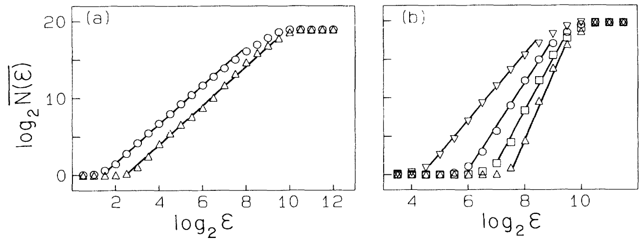

FIG. 4. Plots of $\log_2 \overline{N}(\epsilon)$ vs $\log_2 \epsilon$ used to compute fractal dimension d at $B_0 = 11.15$ kG. (a) $V_{dc} = 12.1$ V, $N = 490\,000$ data points; the circles and triangles refer to embedding dimensions of 4 and 8, respectively. Slopes have converged to 2.5 with respect to both D and N. (b) $V_{dc} = 12.9$ V, $N = 884\,000$; inverted triangles, circles, squares, and triangles refer to $D = 6$, 10, 14, and 18, respectively. Slopes have not converged with respect to either D or N. For $D = 18$, the slope is 8.7.

dimension calculations based on time series taken across different pairs of probe contacts $V_i(t)$ yield the same results as those based on total current $I(t)$, for both spatially coherent and incoherent states. Further, we find that for fixed values of our applied fields, the power spectrum measured across a pair of probe contacts $|V_i(\omega)|^2$ is essentially identical to the power spectrum of the total current $|I(\omega)|^2$. This suggests that the spatial incoherence may be due to the dispersive nature of the eh plasma.

This difficulty in calculating large fractal dimensions is a problem incurred with very chaotic systems.[12] The number of data points required for convergence increases exponentially with the fractal dimension of the system. At present, although we know that our system experiences a large jump in dimensionality at the onset of spatial incoherence, we have not yet determined whether this onset is characterized by chaotic dynamics of an attractor of fractal dimension many orders of magnitude smaller than the number of degrees of freedom of the particles in the system ($\sim 10^{10}$). Other approaches for quantitatively characterizing very chaotic states (say, $d > 10$) will need to be developed before this intriguing question can be answered.

We wish to thank E. E. Haller and the members of his laboratory for the Ge samples and assistance in the sample preparation. Also, we thank J. D. Farmer and J. P. Crutchfield for helpful discussions. This work was supported by the Director, Office of Energy Research, Office of Basic Energy Science, Materials Sciences Division of the U.S. Department of Energy under Contract No. DE-AC03-76SF00098.

[1]For example, see H. L. Swinney, Physica (Utrecht) **7D**, 3 (1983); see also The Physics of Chaos and Related Problems, edited by S. Lundqvist, Phys. Scr. **T9** (1985).

[2]D. Ruelle and F. Takens, Commun. Math. Phys. **20**, 167 (1971); E. Ott, Rev. Mod. Phys. **53**, 655 (1981).

[3]S. Ciliberto and J. P. Gollub, Phys. Rev. Lett. **52**, 922 (1984).

[4]P. S. Lomdahl, A. R. Bishop, O. H. Olsen, and J. C. Eilbeck, Bull. Am. Phys. Soc. **30**, 421 (1985).

[5]I. L. Ivanov and S. M. Ryvkin, Zh. Tekh. Fiz. **28**, 774 (1958) [Sov. Phys. Tech. Phys. **3**, 722 (1958)]; M. Glicksman, Phys. Rev. **124**, 1655 (1961).

[6]C. E. Hurwitz and A. L. McWhorter, Phys. Rev. **134**, A1033 (1964).

[7]G. A. Held, C. Jeffries, and E. E. Haller, Phys. Rev. Lett. **52**, 1037 (1984), and in *Proceedings of the Seventeenth International Conference of Physics Semiconductors, San Francisco, 1984,* edited by D. J. Chadi and W. A. Harrison (Springer-Verlag, New York, 1985), p. 1289.

[8]N. H. Packard, J. P. Crutchfield, J. D. Farmer, and R. S. Shaw, Phys. Rev. Lett. **45**, 712 (1980).

[9]This is the method used by A. Brandstäter *et al.,* Phys. Rev. Lett. **51**, 1442 (1983); see also P. Grassberger and I. Procaccia, Phys. Rev. Lett. **50**, 346 (1983).

[10]For the embedding theorem to be applicable, it is required that $D \geqslant 2d + 1$; see Ref. 1.

[11]T. Misawa and T. Yamada, Jpn. J. Appl. Phys. **2**, 19 (1963).

[12]H. S. Greenside, A. Wolf, J. Swift, and T. Pignataro, Phys. Rev. A **25**, 3453 (1982).